

## Article

# Evaluation of the Skin Permeation-Enhancing Abilities of Newly Developed Water-Soluble Self-Assembled Liquid Crystal Formulations Based on Hexosomes

Wesam R. Kadhum <sup>1,\*</sup>, Gerard Lee See <sup>2</sup>, Muqdad Alhijaj <sup>3,4</sup>, Mustafa M. Kadhim <sup>5</sup> , Florencio Jr. Arce <sup>2</sup>, Ahmed S. Al-Janabi <sup>6</sup> , Reyadh R. Al-Rashidi <sup>7</sup> and Anees A. Khadom <sup>8</sup>

<sup>1</sup> Department of Pharmacy, Kut University College, Kut 52001, Iraq

<sup>2</sup> Pharmaceutical Research and Drug Development Laboratories, Department of Pharmacy, School of Health Care Professions, University of San Carlos, Cebu 6000, Philippines

<sup>3</sup> Department of Pharmaceutics, College of Pharmacy, University of Basrah, Basrah 61004, Iraq

<sup>4</sup> Department of Pharmacy, Al-Kunooze University College, Basrah 61029, Iraq

<sup>5</sup> Department of Pharmaceutics, College of Pharmacy, Al-Farahidi University, Baghdad 10011, Iraq

<sup>6</sup> Department of Chemistry, College of Science, Tikrit University, Tikrit 34001, Iraq

<sup>7</sup> Department of Dentistry, Kut University College, Kut 52001, Iraq

<sup>8</sup> Department of Chemical Engineering, College of Engineering, University of Diyala, Baquba 32001, Iraq

\* Correspondence: wesamrkadhum@gmail.com or wesam.r.kadhum@alkutcollege.edu.iq

Tel.: +964-782-825-5935 or +81-80-9462-0134



**Citation:** Kadhum, W.R.; See, G.L.; Alhijaj, M.; Kadhim, M.M.; Arce, F.J.; Al-Janabi, A.S.; Al-Rashidi, R.R.; Khadom, A.A. Evaluation of the Skin Permeation-Enhancing Abilities of Newly Developed Water-Soluble Self-Assembled Liquid Crystal Formulations Based on Hexosomes. *Crystals* **2022**, *12*, 1238. <https://doi.org/10.3390/cryst12091238>

Academic Editors: Changquan Calvin Sun, Borislav Angelov, Yanzi Gao and Cheng Zou

Received: 14 June 2022

Accepted: 26 August 2022

Published: 1 September 2022

**Publisher's Note:** MDPI stays neutral with regard to jurisdictional claims in published maps and institutional affiliations.



**Copyright:** © 2022 by the authors. Licensee MDPI, Basel, Switzerland. This article is an open access article distributed under the terms and conditions of the Creative Commons Attribution (CC BY) license (<https://creativecommons.org/licenses/by/4.0/>).

**Abstract:** The present study aimed to develop polyethylene glycol–liquid crystals (PEG-LC) ointment formulations, assess their formulation characteristics, and establish their biocompatibility and impact on transdermal drug administration. PEG-LC formulations were prepared using a hydrophilic molecule, *p*-aminobenzoic acid (PAB). Formulation characterizations such as small-angle X-ray scattering, viscosity, pH, zeta potential, and the particle sizes of the formulations were examined to determine the physicochemical properties of the prepared formulations. The drug release profile of PEG-LC ointment formulations was assessed with a dialysis membrane. In vitro skin permeation testing was performed to establish whether the PEG-LC formulations improved drug skin penetration. The MTT and comet assays were performed to assess the biocompatibility of the formulations. Our data showed that the method is effective in forming hexosome-type PEG-LC formulations and that they were biocompatible. Furthermore, the PEG-LC formulations significantly improved PAB skin penetration when compared with commercial PEG. The PEG-LC formulation is a promising carrier for the delivery of hydrophilic drugs.

**Keywords:** *p*-aminobenzoic acid; polyethylene glycol; liquid crystals; formulations; skin penetration

## 1. Introduction

Skin is the external covering or integument of the human body with a surface area of 1.8 m<sup>2</sup> and offers a site for drugs to be delivered into the body due to its easy and convenient accessibility, non-invasive nature, and success in treating localized illnesses. The skin is composed of two major layers, the dermis and the epidermis [1,2]. Furthermore, the stratum corneum (SC) is the top layer of the human skin (epidermis), which serves as the first physical membrane against any foreign substances entering the body, including medications, and presents a substantial difficulty for topical drug delivery systems [2]. Two important properties of an efficient topical formulation are thermodynamic stability and excellent drug partitioning across the skin layers [3].

Ointment is a single-phase semisolid pharmaceutical dosage form that allows for the insertion of either hydrophilic or hydrophobic medicinal components. Ointment dosage forms are designed for topical application, but they have several disadvantages, including limited absorption and a lack of penetration into the stratum corneum. The ideal ointment

formulations are crucial for overcoming the SC. As a result, selecting ointment bases has to be duly considered, as the extent of medication release is determined by the types of ointment bases employed, which impacts the drug's effectiveness [4–8].

Polyethylene glycols (PEGs) are hydrophilic polyether compounds with different applications and physical properties, varying from odorless, colorless, waxy solids to viscous liquids [9–11]. Low-molecular-weight PEGs can be used as eye drops, suppository bases, solvents, and injections. On the other hand, high-molecular-weight PEGs can be used to prepare film coats and tablets. PEGs have been widely used in the pharmaceutical industry and cosmetics; however, it is still challenging to ensure the sufficient penetration of drugs through the skin.

Monoolein's LC phases have intriguing features ideal for medication delivery systems through the skin. Glycerol monoolein (GMO), for example, is a biocompatible and bioadhesive penetration enhancer that can integrate substances regardless of their solubility. Furthermore, sensitive medications can be protected against physical and enzymatic degradation while still being delivered for a long period of time [12]. GMOs in liquid crystal systems have been used in a variety of ways, including transdermal, ocular, oral, and nose-to-brain delivery. Drug absorption after the oral and topical administration of LC formulations is dramatically affected by the concentration of LC. The concentration of LC-forming lipids and the physiochemical properties of entrapped drugs are key issues for the good performance of LC formulations in various pharmaceutical applications [13]. The main advantages of LCs are mainly related to their easy in situ injection as a lamellar phase and their instant in situ transition into a cubic phase. In vivo studies have proven the biocompatibility and the inertia of LCs after their application on the myocardial tissue of mice [14]. An ex vivo study revealed a significant enhancement, up to six-fold, in the transdermal permeation of resveratrol-loaded LCs compared to a suspension [15].

LCs are crystalline, lipid-based semisolids that combine the advantages of both the liquid and crystal states. Glycerol monooleate (GMO) is often described as a self-assembling amphiphilic molecule that plays a very important role in transdermal drug delivery systems; it is a synthetic compound that is considered a monoglyceride (Figure 1).

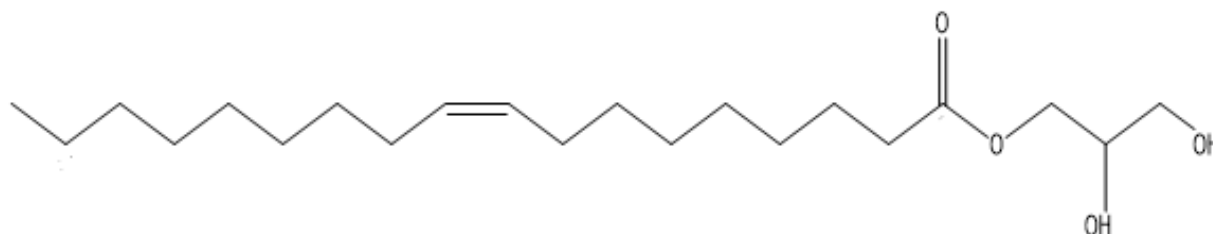


**Figure 1.** Glycerol monooleate (GMO) structure.

GMO is capable of producing inverted micelles with an oily texture in the presence of a small amount of water [16,17]. Hexagonal or cubic phases develop when more water (20–40%) is introduced to GMO over a wide temperature range. With the addition of surfactants, different amphiphilic lipids, such as phytantriol (PHT) or GMO, spontaneously create LC systems in excess amounts of water. The most prevalent phases identified in lyotropic LCs are lamellar, cubic, and hexagonal [18–20]. Hexagonal and cubic phases have gained a lot of interest from scientists because they can be applied as matrices for the slow-release of active drugs of various polarity and molecular sizes and because of their highly ordered inner structures [21,22]. This study is the first to develop PEG-LC formulations incorporating *p*-amino benzoic acid (PAB)—a hydrophilic model drug. PAB was chosen as a chemical since it is a vitamin B complex component that is often used as an antioxidant [23,24]. In addition, dermatomyositis, Peyronie's disease, and scleroderma are conditions that require PAB potassium salt for treatment [25–27]. PAB is currently considered an active ingredient in cosmeceuticals, nutritional supplements, and as a medicine for skin disorders.

The present study aimed to develop polyethylene glycol–liquid crystals (PEG-LC) ointment formulations, assess their formulation characteristics, and establish their biocompatibility and impact on transdermal drug administration. In our previous studies, we emphasized the development of oleaginous bases in LCs [6–8]. However, no studies were carried out to develop a liquid crystal formulation in conjunction with water-soluble ointment bases.

The particle sizes, zeta potential, and viscosities of these formulations were measured to ascertain their physicochemical properties. Small-angle X-ray scattering (SAXS) was applied to detect the hexosome phase structures of the designed formulations. A dialysis membrane was performed to determine the PAB released from PEG-LC formulations. In vitro experiments with Franz diffusion cells showed that LC formulations improve the skin disposition of the drug. The biocompatibility of the prepared formulations was assessed with MTT and comet assays.

## 2. Methods and Materials

### 2.1. Materials

PEG 3350, PEG 400, GMO (>97%), PAB, and Pluronic<sup>®</sup> F127 were obtained from Sigma-Aldrich (St. Louis, MO, USA). Human keratinocytes were obtained from the American Type Culture Collection, Manassas, VA, USA (HaCaT). Other solvents and reagents utilized were of either analytical or HPLC grade and were not purified further.

### 2.2. Optimization of PEG-LC Ointment Formulation

Table 1 lists the PEG-LC ointment formulations prepared in this research. The ingredients were accurately weighed and the GMO was incorporated into the ointment base (PEG 3350 and PEG 400). The prepared formulations were made by changing the amount of GMO (which had previously been melted at 70 °C before usage). PAB was then added to the PEG-LC formulations and homogenized.

**Table 1.** Composition of PEG-LC formulations.

Ingredients (%)	PEG	PEG-GMO10	PEG-GMO20	PEG-GMO30
PEG 3350 (%)	40	40	40	40
PEG 400 (%)	50	40	30	20
GMO (%)	0	10	20	30
Pluronic <sup>®</sup> F127 (%)	1	1	1	1
PAB solution (purified water) (%)	9	9	9	9
Total %	100%	100%	100%	100%

### 2.3. Zeta Potential Measurements and Particle Size

The zeta potential and particle size of PEG-LC ointment formulations were measured by a Zetasizer (Malvern, UK). Prior to analysis, a vortex mixer was utilized to agitate and dilute the PEG-LC samples. Three replicates were used in the measurements.

### 2.4. Viscosity

A viscometer (Alpha Analytical, Westborough, MA, USA, MCR 301) with a viscosity measurement range of 0.3–15,000 mPa·s and a relative error of 1% was applied to measure the viscosity of PEG-LC ointment formulations. The viscosity values of the prepared formulations were measured as a single point against a shear rate of 100 rotations per minute (rpm). Three replicates were used in the measurements.

### 2.5. Small-Angle X-ray Scattering

A nano viewer with a Pilatus (100K/RL 2D) detector was applied to perform SAXS studies on PEG-LC formulations (Anton Paar, Graz, Austria). Cu K radiation with a voltage and current of 45 kV and 110 mA and a wavelength of 1.54 Å was used as the X-ray source.

The distance between the sample and the detector was 375 mm. In a vacuum-resistant glass capillary cell, each sample was heated to 25 °C for ten minutes.

### 2.6. PAB Release Experiment

A dialysis membrane (with an MW of 10 kDa; Thermo Fisher Scientific, Waltham, MA, USA; diffusion area of 0.95 cm<sup>2</sup>) was fixed on a vertical-type Franz diffusion cell with a receiver portion loaded with phosphate-buffered saline (pH 7.4) and was kept at 32 °C. The donor cell was then loaded with 1.0 mL of the PEG-LC formulation. After the preset sampling time, the sample from the receiver chamber was withdrawn and replenished with an equivalent volume of phosphate-buffered saline (500 µL) to maintain the volume of the chamber. The final time for the release experiment was up to 8 h. The amount of permeated PAB was measured using an HPLC instrument.

Various mathematical models were applied to evaluate the release kinetics of PAB from PEG-LC formulations, including zero-order, first-order, Higuchi, and Korsmeyer–Peppas.

$$Q_t = Q_0 + k_0 * t \quad (1)$$

$$\log Q = \log Q_0 - k_1 * t / 2.303 \quad (2)$$

$$Q_t = k_{HC} * t^{1/2} \quad (3)$$

$$M_t / M_\infty = k t^n \quad (4)$$

where

$Q_t$  is the amount of drug released at time  $t$ ;

$Q_0$  is the initial amount of the drug in the formulation;

$k_0$ ,  $k_1$ , and  $k_{HC}$  are release rate constants for zero-order, first-order, and Higuchi model equations;

$M_t$  is the amount of drug released at time  $t$ ;

$M_\infty$  is the amount of drug released at time  $\infty$ ;

$k$  is the kinetic constant;

$n$  is the diffusion coefficient;

The cumulative % of PAB released was fitted using the Higuchi model [28].

### 2.7. Animals

Permeation membrane (i.e., skin) was sourced from 8-week-old male hairless rats. The rats were housed in temperature-controlled rooms (25 ± 2 °C) with a 12 h light–dark cycle (07:00–19:00 h). Food and water were made freely available to the rats. The animal experiment protocol was reviewed by Wasit University's Animal Care and Use Committee.

### 2.8. In Vitro Penetration through the Skin

Abdominal skin was isolated from the abdominal area of the hairless rats under anesthesia (pentobarbital at 50 mg/kg, intraperitoneally). Isolated skin, with the epidermal side upward, was set in a vertical type Franz diffusion cell (effective diffusion area: 0.95 cm<sup>2</sup>). The receiver chamber was loaded with phosphate-buffered saline (pH 7.4) and kept at 32 °C. Prior to applying PEG-LC formulations and commencing the skin penetration studies, a 60 min hydration period with PBS was performed. PBS was then loaded onto the receiver cell similar to the PAB release experiment.

PEG-LC ointment formulations were loaded into the donor chamber (0.1 mL) to begin the in vitro skin disposition study. At the preset sampling schedule, an aliquot of 500 µL was taken from the receiver cell and replaced with the same quantity of PBS thereafter.

In order to determine the skin concentration of PAB, the skin piece (0.1 g) was minced with scissors and homogenized (5 min, 4 °C) with water (0.9 mL) using a homogenizer (Polytron PT-MR 3000; Kinematica Inc., Littau, Switzerland). The homogenate was mixed with acetonitrile:water = 1:1 (0.5 mL) and agitated for 15 min. After centrifugation (5 min, 4 °C), the supernatant (50 µL) was mixed with the same volume of acetonitrile containing

methylparaben (10 µg/mL) and centrifuged again (5 min, 4 °C). The obtained supernatant (20 µL) was injected into an HPLC system.

### 2.9. HPLC Conditions

PAB samples (50 µL) were mixed with the same quantity of the internal standard (acetonitrile containing methylparaben). After centrifugation, the supernatant (20 µL) was then injected into an HPLC system composed of a pump (LC-20AD), column oven (CTO-20A), auto-sampler (SIL-20AC), system controller (CBM-20A), and UV detector (SPD-M20A). A reverse phase column (ODS-3 5µm, 4.6 × 250 mm) was used in the analysis of PAB, maintained at 40 °C (GL Sciences Inc., Atlanta, GA, USA). As for the mobile phase, acetonitrile (0.1 percent phosphoric acid = 0–4 min (8:52), 4–14 min (35:65), and 14–20 min (8:92)) was used at 1 mL per minute flow rate. PAB was measured at UV 280 nm [13].

### 2.10. MTT Assay

PEG-LC formulations were tested for their skin safety on human epidermal keratinocytes using HaCaT. Cells were cultivated at a density of  $8 \times 10^3$  cells per well (96-well plates) and incubated for 24 h. PEG-LC formulations were diluted (0.1, 0.5, and 1 mg/mL) in growth medium and were added to the well. For 12 and 24 h, the cells were subjected to PEG-LC formulations. After that, the wells were filled with MTT mixed with DMEM (0.5 mg/mL) and incubated for 4 h at 37 °C [29].

### 2.11. DNA Damage Assessment (Comet Assay)

In a multi-well configuration, cells were plated at a density of  $4 \times 10^5$  cells/mL of culture media. After 24 h of development, cells were exposed to various doses of PEG-LC formulations (0.1–1 mg/mL), as well as 50 µM H<sub>2</sub>O<sub>2</sub> as a positive control. The cells were washed in PBS and treated with 300 L of trypsin, incubated for 3 min, and then transferred to 1 mL of DMEM + 10% FBS medium after 24 h. The cells were separated by pipetting. In Eppendorf tubes, the cell suspension was centrifuged for 3 min at 1000 rpm. After the supernatant was removed, the cells were resuspended in 100 L of PBS (kept on ice).

On see-through slides (frosted), a first layer of 0.6 percent normal melting agarose (NMA) coating was applied, followed by a second layer of cell suspension and 0.6 percent low melting agarose (LMA) and a third layer of 0.6 percent LMA (without cell). Then, a lysing solution containing NaCl (2.5 M), Na<sub>2</sub>EDTA (100 mM), Tris (10 mM), and Triton-X (1%) was added for 1 h and the slides were placed in a horizontal electrophoresis tank. After that, electrophoresis at 0.3 A and 25 V was performed (20 min). Before being inspected with a fluorescence microscope, the slides were stained with ethidium bromide and stored in a humidified airtight container. The degree of DNA damage was visually classified into five categories based on the amount of DNA in the tail [29].

## 3. Results and Discussion

The delivery of hydrophilic drugs (e.g., PAB, ibuprofen) through the skin using semisolid transdermal preparations (i.e., ointments) is considered challenging owing to their complex physicochemical properties and the tortuous route through the structure of the skin. PAB alone poorly penetrates the skin, which limits its clinical efficacy.

This study employed product profile identification and characterization to select the PEG-LC formulations for investigation. First, the physical stability and homogeneity of the PEG-LC formulations were assessed (Table 1). Formulations with a non-uniform appearance exhibiting phase separation were rejected, while those formulations presenting a homogeneous and opaque appearance with no visible aggregations were accepted. Increasing the GMO concentration to 30% (PEG-GMO30) resulted in a non-uniform, highly viscous mixture with apparent phase separation. Furthermore, applying these formulations topically proved problematic. As a result, no further investigation on this formulation was conducted.

The pH, particle size, zeta potential, and viscosity values of the topical PEG-LC ointment formulations are presented in Table 2. The findings suggest that, at high GMO concentrations, particle sizes decrease and the negatively charged zeta potential increases. The zeta potential is a parameter that is applied to measure the stability and biodistribution of a formulation [30]. High surface charges prevent particles from aggregating by producing repulsion forces among them [31]. Because of the existence of free oleic acid in the prepared formulations, the particles may have had a negative charge resulting in negative zeta potential values. Furthermore, the hydroxyl ion preferential adsorption at the lipid–water interface can explain the negative charge [6]. The results of the viscosity tests demonstrated that the amount of GMO in the formulation had a significant impact on these values. As the GMO concentration in the PEG-LC formulations increased, so did the viscosity. Increasing the GMO concentration used in the formulation had a significant effect on the viscosity of the PEG-LC ointment formulations, indicating that viscosity rose as LC-forming lipid content increased. These results were consistent with previous studies on LC formulations [22]. The prepared LC formulations had pH values similar to that of the skin.

**Table 2.** Determination of particle size, viscosity, pH, and zeta potential.

Formulation	Particle Size (nm)	Viscosity (mPa.s)	pH	Zeta Potential (mV)
PEG	602 ± 35	8201 ± 261	4.9 ± 0.4	−14 ± −2
PEG-GMO10	520 ± 29	9822 ± 403	5.3 ± 0.6	−20 ± −3
PEG-GMO20	411 ± 22	1139 ± 557	5.6 ± 0.5	−26 ± −2

The phase structure of the prepared ointment formulations was investigated with SAXS. The X-ray diffraction characteristics of PEG-GMO10 and PEG-GMO20 formulations are shown in Figure 2. In the prepared formulations, the existence of the hexagonal phase (H2 inverted) was shown with reflection patterns at about 1,  $\sqrt{3}$ , and  $\sqrt{4}$ . These results demonstrated that PEG-LC formulations successfully managed to form hexosome-type liquid crystals.

The release kinetics of PAB from the PEG-LC formulations was evaluated using the four models (zero-order, first-order, Korsmeyer–Peppas, and Higuchi) that are often used to describe the phenomenon (Table 3).

**Table 3.** Release kinetics models used to describe the release of PAB from PEG-LC formulations.

Formulation	Zero-Order	First-Order	Korsmeyer–Peppas Model	Higuchi Model
	Regression Coefficient R <sup>2</sup>			
PEG	0.932	0.891	0.789	0.993
PEG-GMO10	0.921	0.772	0.767	0.989
PEG-GMO20	0.958	0.833	0.883	0.979

The fitting factor (R<sup>2</sup>) values in the four models were in the following order: Higuchi > zero-order > first-order > Korsmeyer–Peppas (suitable for PEG-LC formulations). PAB release profiles from the PEG-LC formulations were determined using Higuchi’s model.

Figure 3 depicts the PAB release characteristics from the PEG-GMO10 and PEG-GMO20 LC formulations. The amount of PAB released from the PEG-GMO10 and PEG-GMO20 formulations was 12.5 and 8.6 percent, respectively, suggesting that, when GMO concentration is increased, the amount of PAB released from the formulation decreases. As shown in Figure 3, the content of GMO had an effect on the PAB release profiles of the prepared formulations. PAB diffusivity from the formulation decreased as the GMO concentration increased.

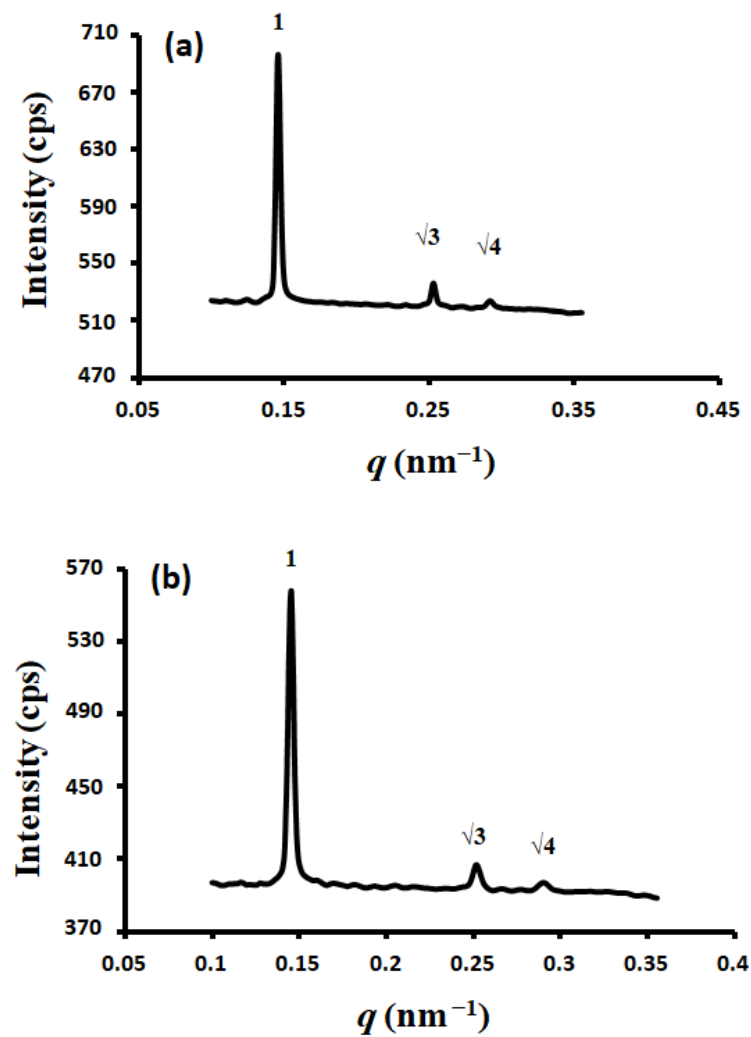


Figure 2. SAXS charts of PEG-GMO10 (a) and PEG-GMO20 (b) formulations.

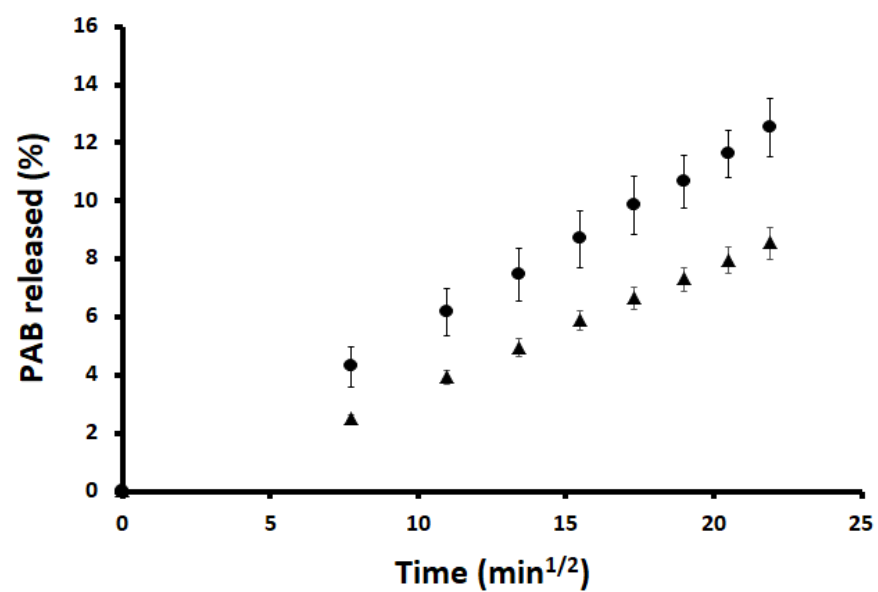
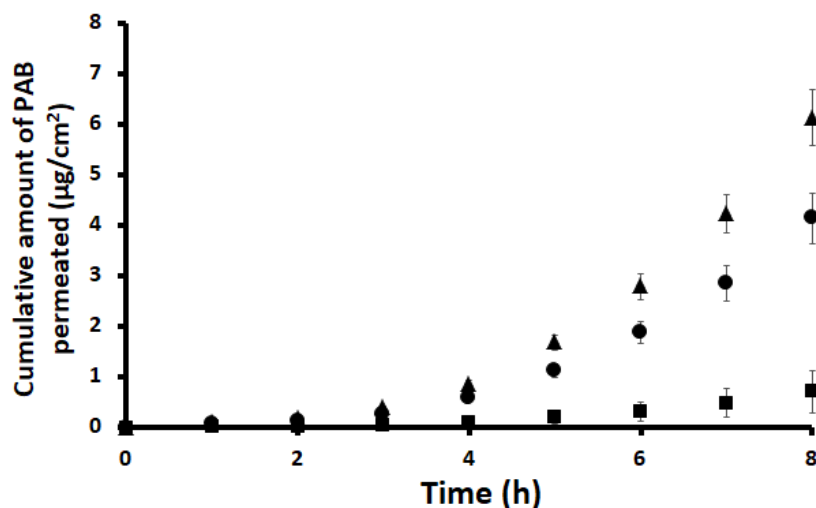


Figure 3. PAB release profiles: (●), PEG-GMO10 formulation; (▲), PEG-GMO20 formulation. Each point is the mean  $\pm$  S.E. of three experiments.

Figure 4 depicts the effect of PEG-GMO10 and PEG-GMO20 LC formulations on PAB that permeated through hairless rat skin. PEG-GMO10 and PEG-GMO20 dramatically enhanced the permeation of PAB when compared with PEG alone—a chemical permeation enhancer. At 8 h, the PEG-GMO10 and PEG-GMO20 formulations increased skin penetration rates by 8.7- and 5.8-fold, respectively.



**Figure 4.** The effect of PEG-GMO formulations on the cumulative amount of PAB over time. (■), PEG alone; (●), PEG-GMO10 formulation; (▲), PEG-GMO20 formulation. Each point represents the mean  $\pm$  S.E. of three experiments.

The results of *in vitro* skin penetration were significantly influenced by the GMO concentration (Figure 4). The skin permeation of PAB was dramatically improved in formulations of 10% (PEG-GMO10) and 20% GMO (PEG-GMO20). These results clarified that PEG-LC ointment formulations are better than commercial PEG alone in terms of improving skin permeability.

The effect of GMO on the skin deposition of PAB in the deeper layers of the skin, such as the viable epidermis, was confirmed by our experiments. PAB concentration in the skin (at 8 h) following the application of the PEG-LC formulations (expressed as the amount ( $\mu\text{g}$ ) of drug per gram of skin) is shown in Figure 5. PAB skin concentrations were significantly greater in skin samples treated with PEG-GMO10 and PEG-GMO20 formulations than in skin samples treated with PEG.

As a result, a significant increase in the skin deposition of PAB was confirmed after the application of PEG-GMO formulations. The exact mechanism by which LC systems increase skin permeability is not fully understood [32]. However, a recent study described how the hexagonal phases of LCs are capable of promoting LC fusion with the SC and the deeper layers of the skin, resulting in enhanced drug delivery into the skin. Previous studies have established a number of hexagonal phase advantages, such as high fluidity, a large surface area for interaction with biological barriers, and allowing for higher amounts of drugs to be incorporated regardless of solubility. To fully comprehend the mechanism of LC phase structures in drug penetration through the skin, more investigation is required [33,34].

The biocompatibility of PEG-GMO formulations was also investigated using HaCaT (Figure 6). PEG-GMO10 and PEG-GMO20 (0.1–1 mg/mL) were added to the HaCaT cells at varied doses (Figure 6a,b). The HaCaT cell viability was >98% at different concentrations of the prepared formulations. The PEG LC formulations' safety on HaCaT cells was also proven at a higher dose, 1 mg/mL, where cell survival was >90%. Prior studies using human keratinocytes to examine the safety of various recently manufactured formulations [35,36] support our findings.

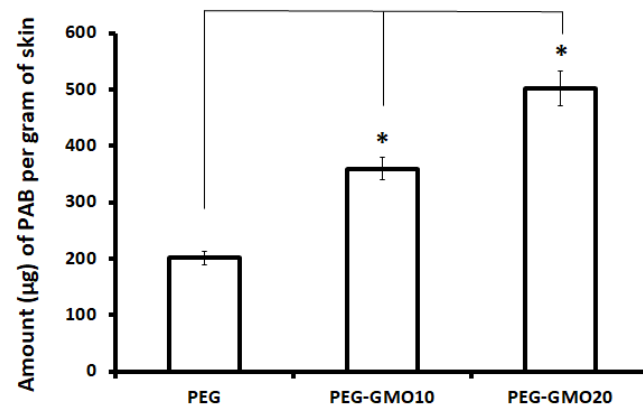


**Figure 5.** PAB accumulation in the skin (expressed as the amount (µg) of PAB per gram of skin) following 8 h of treatment with PEG, PEG-GMO10, and PEG-GMO20 formulations. Each column reflects the mean  $\pm$  S.E. of three experiments. \*:  $p < 0.05$  significantly different from PEG (Student's  $t$ -test).

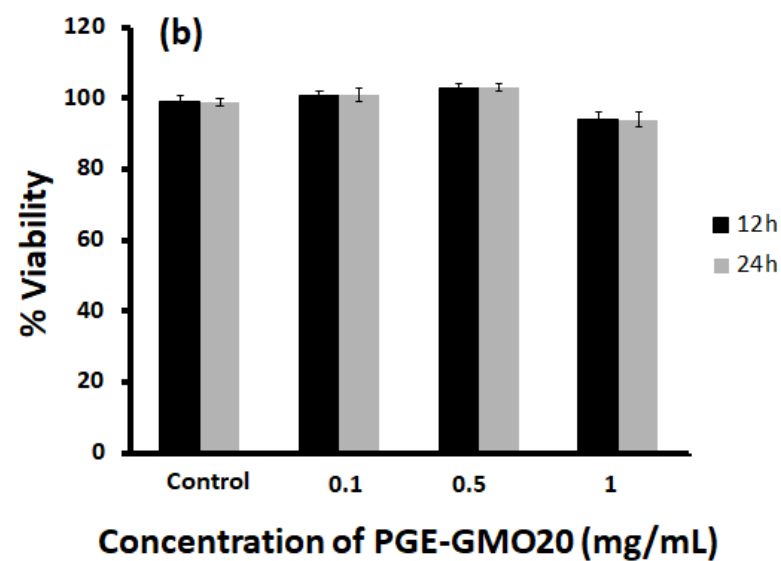
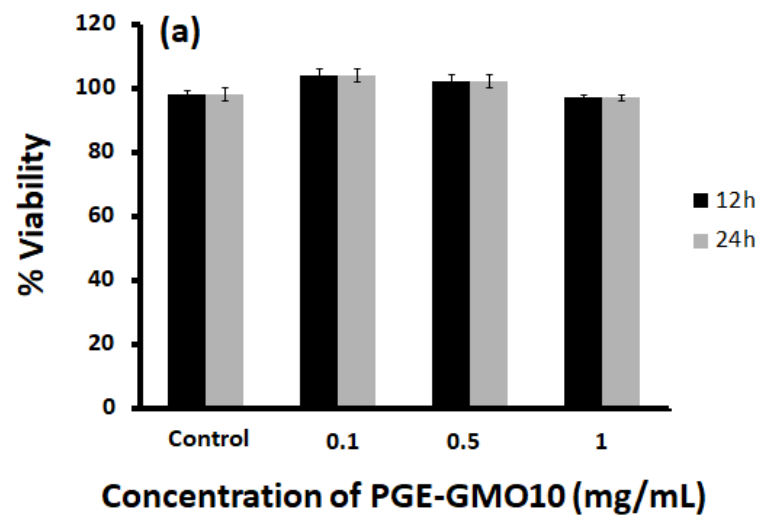


**Figure 6.** Cell viability of HaCaT cells after incubation with PEG-GMO10 (a) and PEG-GMO20 (b) formulations at different concentrations for 12 h and 24 h, respectively.

Furthermore, even at 1 mg/mL, the PEG-GMO formulations had no genotoxic response against HaCaT cells (Tables 4 and 5) according to our findings (Figure 7).

**Table 4.** Effect of PEG-GMO10 formulation on DNA damage in HaCaT cells estimated with the comet assay.

Grade of Genotoxicity	Control	50 $\mu$ M H <sub>2</sub> O <sub>2</sub>	0.1 mg/mL	0.5 mg/mL	1 mg/mL
Grade 0	99	15	96	93	95
Grade 1	1	17	2	6	3
Grade 2	0	10	1	1	2
Grade 3	0	28	1	0	0
Grade 4	0	30	0	0	0

**Table 5.** Effect of PEG-GMO20 formulation on DNA damage in HaCaT cells estimated with the comet assay.

Grade of Genotoxicity	Control	50 $\mu$ M H <sub>2</sub> O <sub>2</sub>	0.1 mg/mL	0.5 mg/mL	1 mg/mL
Grade 0	97	20	97	91	93
Grade 1	2	12	1	8	5
Grade 2	1	6	1	1	1
Grade 3	0	30	1	0	1
Grade 4	0	32	0	0	0

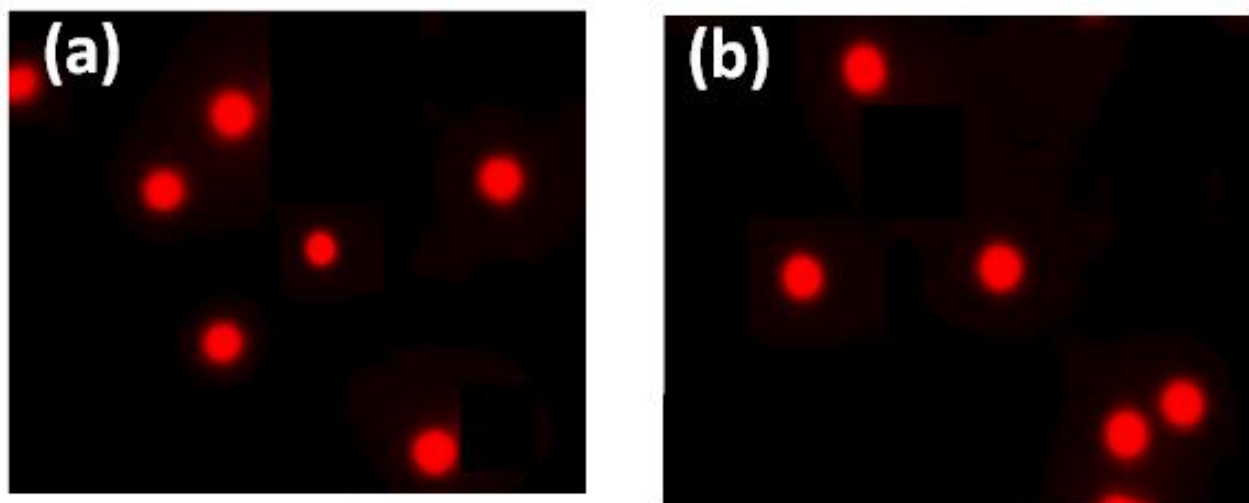


**Figure 7.** Comet assay images of HaCaT cell lines treated with 1 mg/mL of PEG-GMO10 formulation (a) and 1 mg/mL of PEG-GMO20 formulation (b).

Human keratinocytes treated with hydrogen peroxide (50  $\mu$ M) caused considerable DNA damage as a positive control (grade 3, grade 4). The results also demonstrated that treating HaCaT cells with PEG-GMO10 and PEG-GMO20 at 1 mg/mL does not cause significant DNA damage (Figure 7), suggesting that PEG-LC formulations are safe for medicinal applications.

The current study demonstrates how biocompatible materials such as GMO and PEG can be used to generate hexosome- or cubosome-type LC formulations. Temperature, LC lipid type, the physiochemical properties of drug, lipid content, and surfactant type were all hypothesized to influence the phase structure and the performance of LC ointment formulations.

#### 4. Conclusions

The current investigation demonstrated that the PEG-GMO is capable of delivering hydrophilic drugs into the skin at a higher drug payload with GMO acting as a skin permeation enhancer. The preparation of an ointment base with PEG and GMO effectively formed hexosome-type liquid crystal formulations. In vitro skin permeation results clearly showed that the PEG-LC formulations significantly improved PAB skin penetration when compared with commercial PEG. Formulation characterizations such as small-angle X-ray scattering, viscosity, pH, zeta potential, and the particle sizes of the formulations were examined to determine the physicochemical properties of the prepared formulations. More investigation is required to fully comprehend the mechanism of LC phase structures on drug penetration through the skin. The MTT and comet assays were performed to assess the biocompatibility of the formulations. The PEG-LC formulations were biocompatible with human epidermal keratinocytes (HaCaT). The PEG-LC formulation is a promising carrier for the transdermal delivery of hydrophilic drugs.

**Author Contributions:** Conceptualization, W.R.K., G.L.S. and M.A.; methodology, W.R.K., G.L.S., R.R.A.-R. and F.J.A.; software, R.R.A.-R.; validation, W.R.K., M.M.K. and G.L.S.; formal analysis, W.R.K.; investigation, A.S.A.-J. and R.R.A.-R.; data curation, A.S.A.-J. and F.J.A.; writing—original draft preparation, W.R.K.; writing—review and editing, G.L.S., A.A.K., F.J.A., M.M.K. and A.S.A.-J.; visualization, M.M.K. and A.A.K. All authors have read and agreed to the published version of the manuscript.

**Funding:** This research received no external funding.

**Institutional Review Board Statement:** This study was reviewed and approved (F-77536) by Kut University college and University of Basrah.

**Informed Consent Statement:** Not applicable.

**Data Availability Statement:** The data that support the findings of this study are available from the corresponding author, [Wesam R. Kadhum], upon reasonable request.

**Conflicts of Interest:** The authors declare no conflict of interest.

#### References

1. Kirschner, N.; Brandner, J.M.; Ann, N.Y. Barriers and more: Functions of tight junction proteins in the skin. *Ann. N. Y. Acad. Sci.* **2015**, *1257*, 158–166. [[CrossRef](#)] [[PubMed](#)]
2. Alkilani, A.; McCrudd, M.; Donnelly, R. Transdermal Drug Delivery: Innovative Pharmaceutical Developments Based on Disruption of the Barrier Properties of the Stratum Corneum. *Pharmaceutics* **2015**, *7*, 438–470. [[CrossRef](#)] [[PubMed](#)]
3. Singhal, M.; Lapteva, M.; Kalia, Y. Formulation challenges for 21st century topical and transdermal delivery systems. *Expert Opin. Drug Deliv.* **2017**, *14*, 705–708. [[CrossRef](#)] [[PubMed](#)]
4. Shelke, U.Y.; Mahajan, A.A. Review on: An Ointment. *Int. J. Pharm. Pharm. Res.* **2015**, *4*, 171–176.
5. Francis, A.O.; Ezekiel, O.A.; Abiola, I.R.; Gbemisola, O.A.; Victor, O.B. Evaluation of topical antimicrobial ointment formulations of essential oil of lippia multiflora moldenke. *J. Tradit. Complementary Altern. Med.* **2015**, *135*, 135–144.
6. Lu, Y.; Xiao, Y.; Yin, M.-Z.; Zhou, X.-C.; Wu, L.-S.; Chen, W.-Q.; Kuang, Y.-H.; Zhu, W. Polyethylene Glycol Ointment Alleviates Psoriasis-Like Inflammation Through Down-Regulating the Function of Th17 Cells and MDSCs. *Front. Med.* **2021**, *7*, 560579. [[CrossRef](#)]
7. Jang, H.J.; Shin, C.Y.; Kim, K.B. Safety Evaluation of Polyethylene Glycol (PEG) Compounds for Cosmetic Use. *Toxicol. Res.* **2015**, *31*, 105–136. [[CrossRef](#)]
8. Di Palma, J.A.; De Ridder, P.H.; Orlando, R.C.; Kolts, B.E.; Cleveland, M.B. A randomized, placebo-controlled, multicenter study of the safety and efficacy of a new polyethylene glycol laxative. *Am. J. Gastroenterol.* **2000**, *95*, 446–450. [[CrossRef](#)]
9. Hiwale, P.; Lampis, S.; Murgia, S.; Monduzzi, M. Liquid-crystal based formulations for topical drug delivery. *J. Dispers. Sci. Technol.* **2013**, *34*, 1286–1293. [[CrossRef](#)]
10. See, G.L.; Arce, F.J.; Dahlizar, S.; Okada, A.; Fadli, M.F.B.M.; Hijikuro, I.; Itakura, S.; Katakura, M.; Todo, H.; Sugibayashi, K. Enhanced nose-to-brain delivery of tranilast using liquid crystal formulations. *J. Control Rel.* **2020**, *325*, 1–9. [[CrossRef](#)]
11. Chen, Y.; Ma, P.; Gui, S. Cubic and Hexagonal Liquid Crystals as Drug Delivery Systems. *BioMed Res. Int.* **2014**, *2014*, 815981. [[CrossRef](#)] [[PubMed](#)]
12. Kadhum, W.R.; Al-Zuhairy, S.A.S.; Mohamed, M.B.M.; Abdulrahman, A.Y.; Kadhim, M.M.; Alsadoon, Z.; Teoh, T.C. A Nanotechnology Approach for Enhancing the Topical Drug Delivery by Newly Developed Liquid Crystal Formulations. *Int. J. Drug Deliv. Technol.* **2021**, *3*, 716–720.

13. Kadhum, W.R.; Hada, T.; Hijikuro, I.; Todo, H.; Sugibayashi, K. Development and optimization of orally and topically applied liquid crystal drug formulations. *J. Oleo Sci.* **2017**, *66*, 939–950. [[CrossRef](#)] [[PubMed](#)]
14. Mancuso, A.; Cianflone, E.; Cristiano, M.C.; Salerno, N.; Tarsitano, M.; Marino, F.; Molinaro, C.; Fresta, M.; Torella, D.; Paolino, D. Lyotropic Liquid Crystals: A Biocompatible and Safe Material for Local Cardiac Application. *Pharmaceutics* **2022**, *14*, 452. [[CrossRef](#)]
15. Badie, H.; Abbas, H. Novel small self-assembled resveratrol-bearing cubosomes and hexosomes: Preparation, characterization, and ex vivo permeation. *Drug Dev. Indust. Pharm.* **2018**, *44*, 2013–2025. [[CrossRef](#)]
16. Ganem-Quintanar, A.; Quintanar-Guerrero, D.; Buri, P. Monoolein: A review of the pharmaceutical applications. *Drug Dev. Indust. Pharm.* **2000**, *26*, 809–820. [[CrossRef](#)]
17. Kadhum, W.R.; Oshizaka, T.; Hijikuro, I.; Todo, H.; Sugibayashi, K. Usefulness of liquid-crystal oral formulations to enhance the bioavailability and skin tissue targeting of p-aminobenzoic acid as a model compound. *Eur. J. Pharm. Sci.* **2016**, *88*, 282–290. [[CrossRef](#)]
18. Kadhum, W.R.; Todo, H.; Sugibayashi, K. Skin permeation: Enhancing ability of liquid crystal formulations. In *Percutaneous penetration Enhancers Chemical Methods in Penetration Enhancement: Drug Manipulation Strategies and Vehicle Effects*; Dragicevic-Curic, N., Maibach, H., Eds.; Springer: Berlin/Heidelberg, Germany, 2015; pp. 243–253.
19. Drummond, C.J.; Fong, C. Surfactant self-assembly objects as novel drug delivery vehicles. *Curr. Opin. Colloid Interface Sci.* **1999**, *4*, 449–456. [[CrossRef](#)]
20. Sugibayashi, K.; Todo, H.; Kadhum, W.R. In vitro and in silico approaches to evaluate usefulness and safety of chemical compounds applied or exposed on skin. *Yakugaku Zasshi J. Pharm. Soc. Jpn.* **2014**, *134*, 27–32. [[CrossRef](#)]
21. Kadhum, W.R.; Sekiguchi, S.; Hijikuro, I.; Todo, H.; Sugibayashi, K. A novel chemical enhancer approach for transdermal drug delivery with C17-monoglycerol ester liquid crystal-forming lipid. *J. Oleo Sci.* **2017**, *66*, 443–454. [[CrossRef](#)]
22. Sonja, S.; Nikola, G.; Robert, Z.; Wolfgang, S. Oxidation of ortho- and para-amino benzoic acid. A pulse radiolysis-and gamma radiolysis study. *Radiat. Phys. Chem.* **2010**, *80*, 932–936.
23. Akberova, S.I. New biological properties of p-aminobenzoic acid. *Biol. Bull.* **2002**, *29*, 390–393. [[CrossRef](#)]
24. Rashmi, S.S.; Raechel, C.J.; Carol, J.B.; Mario, G.F.; Alexei, P.L.; Megan, A.M. Effects of Para-Aminobenzoic Acid (PABA) form and administration mode on PABA recovery in 24-Hour Urine Collections. *J. Acad. Nutr. Diet.* **2013**, *114*, 458–463.
25. Zarafonetis, C.J.; Dabich, L.; Skovronski, J.J. Retrospective studies in scleroderma: Skin response to potassium para-aminobenzoate therapy. *Clin. Exp. Rheumatol.* **1988**, *6*, 261–268. [[PubMed](#)]
26. Zarafonetis, C.J.; Dabich, L.; Negri, D. Retrospective studies in scleroderma: Effect of potassium para-aminobenzoate on survival. *J. Clin. Epidemiol.* **1988**, *41*, 193–205. [[CrossRef](#)]
27. Higuchi, T. Mechanism of sustained action medication: Theoretical analysis of the rate of release of solid drugs dispersed in solid matrices. *J. Pharm. Sci.* **1963**, *52*, 1145–1148. [[CrossRef](#)]
28. Wesam, R.K.; Ghanya, A.N.; Mizaton, H.H.; Ilham, M.; Aishah, A. Assessment of genotoxicity and cytotoxicity of standardized aqueous extract from leaves of *Erythroxylumcuneatum* in human HepG2 and WRL68 cells line. *Asian Pac. J. Trop. Med.* **2013**, *10*, 811–816. [[CrossRef](#)]
29. Eman, A.; Shereen, A.Y.; Michael, N.P.; Krishna, T.; Yousuf, H.M.; Sarika, N.; Michael, S.R. Skin models for the testing of transdermal drugs. *Clin. Pharmacol. Adv. Appl.* **2016**, *8*, 163–176.
30. Sherif, S.; Bendas, E.R.; Badawy, S. The clinical efficacy of cosmeceutical application of liquid crystalline nanostructured dispersions of alpha lipoic acid as anti-wrinkle. *Eur. J. Pharm. Biopharm.* **2014**, *86*, 251–259. [[CrossRef](#)]
31. Weiss, V.M.; Naolou, T.; Hause, G.; Kuntsche, J.; Kressler, J.; Mader, I. Poly (glycerol adipate)-fatty acid esters as versatile nanocarriers: From nanocubes over ellipsoids to nanospheres. *J. Control. Release* **2012**, *158*, 156–164. [[CrossRef](#)]
32. Siekmann, B.; Bunjes, H.; Koch, M.H.J.; Westesen, K. Preparation and structural investigations of colloidal dispersions prepared from cubic monoglyceride/water phases. *Int. J. Pharm.* **2002**, *244*, 33–43. [[CrossRef](#)]
33. Esposito, E.; Eblovi, N.; Rasi, S.; Drechsler, M.; di Gregorio, G.; Menegatti, E.; Cortesi, R. Lipid-based supramolecular systems for topical application: A preformulatory study. *AAPS PharmSciTech.* **2003**, *5*, 1–15. [[CrossRef](#)] [[PubMed](#)]
34. Uchino, T.; Murata, A.; Miyazaki, Y.; Oka, T.; Kagawa, Y. Glyceryl monooleyl ether-based liquid crystalline nanoparticles as a transdermal delivery system of flurbiprofen: Characterization and in vitro transport. *Chem. Pharm. Bull.* **2015**, *63*, 334–340. [[CrossRef](#)] [[PubMed](#)]
35. Morganti, P.; Fusco, A.; Paoletti, I.; Perfetto, B.; del Ciotto, P.; Palombo, M.; Chianese, A.; Baroni, A.; Donnarumma, G. Anti-Inflammatory, Immunomodulatory, and Tissue Repair Activity on Human Keratinocytes by Green Innovative. *Nanocomposites Mater.* **2017**, *10*, 843. [[CrossRef](#)] [[PubMed](#)]
36. Al-Zuhairy, S.A.; Kadhum, W.R.; Alhijaj, M.; Kadhim, M.M.; Al-Janabi, A.S.; Salman, A.W.; Al-Sharifi, H.K.; Khadom, A.A. Development and Evaluation of Biocompatible Topical Petrolatum-liquid Crystal Formulations with Enhanced Skin Permeation Properties. *J. Oleo Sci.* **2022**, *71*, 459–468. [[CrossRef](#)]